Original Article

The Rab GTPase-Activating Protein AS160 Integrates Akt, Protein Kinase C, and AMP-Activated Protein Kinase Signals Regulating GLUT4 Traffic

Farah S.L. Thong, Philip J. Bilan, and Amira Klip

Insulin-dependent phosphorylation of Akt target AS160 is required for GLUT4 translocation. Insulin and platelet-derived growth factor (PDGF) (Akt activators) or activation of conventional/novel (c/n) protein kinase C (PKC) and 5′ AMP-activated protein kinase (AMPK) all promote a rise in membrane GLUT4 in skeletal muscle and cultured cells. However, the downstream effectors linking these pathways to GLUT4 traffic are unknown. Here we explore the hypothesis that AS160 is a molecular link among diverse signaling cascades converging on GLUT4 translocation. PDGF and insulin increased AS160 phosphorylation in CHO-IR cells. Stimuli that activate c/n PKC or AMPK also elevated AS160 phosphorylation. We therefore examined if these signaling pathways engage AS160 to regulate GLUT4 traffic in muscle cells. Nonphosphorylatable AS160 (4P-AS160) virtually abolished the net surface GLUT4*myc* gains elicited by insulin, PDGF, K^+ depolarization, or 5-aminoimidazole-4-carboxamide-1-β-D-ribofuranoside but partly, yet significantly, inhibited the effects of 4-phorbol-12-myristate-13-acetate. However, the hypertonicity or 2,4-dinitrophenol–dependent gains in surface GLUT4*myc* were unaffected by 4P-AS160. RK-AS160 (GTPase-activating protein [GAP] inactive) or 4PRK-AS160 (GAP inactive, nonphosphorylatable) had no effect on surface GLUT4*myc* elicited by all stimuli. Collectively, these results indicate that activation of Akt, c/n PKC, or α2-AMPK intersect at AS160 to regulate GLUT4 traffic, as well as highlight the potential of AS160 as a therapy target to increase muscle glucose uptake. *Diabetes* 56:414–423, 2007

Insulin coupling to its receptor activates multiple signaling cascades to elicit its metabolic actions. In particular, activation of phosphatidylinositol-3-kinase (PI3K), Akt, and atypical protein kinase C (PKC) by insulin is essential for elevating GLUT4 at the plasma membrane and for glucose uptake (1). AS160 was recently identified as an Akt substrate (2) and is critically involved in insulin regulation of GLUT4 traffic in 3T3-L1 adipocytes (3–6). AS160 has a GTPase-activating protein (GAP) domain with an essential arginine at position 973 (2) that exhibits GAP activity toward Rabs 2, 8, 10, and 14 (7). Insulin increases AS160 phosphorylation in 3T3-L1 adipocytes (2) and skeletal muscle (8,9). Interestingly, Akt and AS160 phosphorylation are impaired in skeletal muscle obtained from insulin-resistant patients (9) and by the proinflammatory cytokine tumor necrosis factor-α (10). It is currently hypothesized that in the basal state, the GAP activity of AS160 maintains its target Rab in an inactive, GDP-bound form, consequently retaining GLUT4 in intracellular compartment(s) (3–6). Upon insulin stimulation, Akt phosphorylation of AS160 deactivates its GAP activity, shifting the equilibrium of the target Rab to an active GTP-bound form, thereby relieving an inhibitory effect on GLUT4 traffic (3,4). Insulin causes 14-3-3 binding to phosphorylated AS160 and its dissociation from GLUT4 vesicles (11).

In addition to insulin, platelet-derived growth factor (PDGF), which also increases Akt phosphorylation, stimulates GLUT4 exocytosis and glucose transport in cells with an endogenous PDGF receptor (12) or through ectopic expression (13). Also, exercise/contraction, K^+ depolarization (14), or a rise in intracellular Ca^{2+} levels (15) all increase surface GLUT4 levels and glucose uptake in skeletal muscle and cultured muscle cells. In addition, altering metabolic homeostasis with hyperosmotic shock (12,16,17), hypoxia (18,19), and the mitochondrial uncoupler 2,4-dinitrophenol (DNP) (14,16) all elicit an increase in surface GLUT4 density and glucose uptake. However, unlike insulin, the signaling cascades that mediate the effects of muscle contraction and metabolic stressors are independent of the PI3K/Akt pathway and may partially rely on activation of 5′ AMP-activated protein kinase (AMPK), Ca^{2+}/calmodulin kinase (CaMK), and/or selective PKC isoforms (20). With the exception of insulin and PDGF, all of the aforementioned stimuli increase AMPK phosphorylation (14,17). However, AMPK activity is essential only for hypoxia and DNP to promote GLUT4 externalization and glucose uptake (14,19). Conversely, the K^+ depolarization–induced gain in surface GLUT4 does not require AMPK or CaMK-II; instead, it requires intracellular Ca^{2+} and is likely mediated by activation of conventional/novel (c/n) PKC (14,21).

Although AS160 is a downstream effector of the PI3K/Akt axis for insulin stimulation of GLUT4 translocation, the distal effectors of non–insulin-dependent activation of Akt and of the multiple PI3K/Akt-independent signaling

From the Programme in Cell Biology, The Hospital for Sick Children, Toronto, Ontario, Canada.

Address correspondence and reprint requests to Amira Klip, PhD, Programme in Cell Biology, The Hospital for Sick Children, 555 University Ave., Toronto, Ontario, Canada M5G 1X8. E-mail: amira@sickkids.ca.

Received for publication 1 July 2006 and accepted in revised form 2 November 2006.

AICAR, 5-aminoimidazole-4-carboxamide-1-β-D-ribofuranoside; AMPK, AMP-activated protein kinase; BIM, bisindolylmaleimide; CaMK, Ca^{2+}/calmodulin kinase; c/n, conventional/novel; DNP, 2,4-dinitrophenol; GAP, GTPase-activating protein; HA, hemagglutinin; PDGF, platelet-derived growth factor; PI3K, phosphatidylinositol-3-kinase; PKC, protein kinase C; PMA, 4-phorbol-12-myristate-13-acetate.

DOI: 10.2337/db06-0900

cascades that can increase GLUT4 at the plasma membrane are largely unknown. Recently, muscle contraction/exercise (8,22) and chemically activating AMPK with 5-aminoimidazole-4-carboxamide-1-β-D-ribofuranoside (AICAR) (8) were shown to increase AS160 phosphorylation in isolated rodent muscle. However, it is not known if AMPK activation engages AS160 to increase glucose uptake/GLUT4 translocation.

Here we test the hypothesis that AS160 integrates signaling from the Akt, c/n PKC, and AMPK pathways to increase surface GLUT4 content. L6 muscle cells stably expressing *myc*-tagged GLUT4 were used to score surface GLUT4 levels. The entire GLUT4*myc* cohort recycles from intracellular compartments to the membrane in the basal state, and this is accelerated by insulin to the same extent in L6 myoblasts and myotubes. The suitability of L6 GLUT4*myc* myoblasts as a model for studying GLUT4 traffic is extensively reviewed in ref. 23. Here, transfection of AS160 mutants was used to assess the contribution of this protein to GLUT4 traffic in cells challenged by stimuli that activate Akt, c/n PKC, or AMPK. The results suggested that AS160 is a common element in GLUT4 regulation through these three independent signaling pathways.

RESEARCH DESIGN AND METHODS

cDNA plasmids. Plasmids encoding FLAG-tagged wild-type AS160 (WT-AS160), AS160 with four of its six predicted Akt phosphorylation sites (Ser^{318}, Ser^{588}, Thr^{642}, and Ser^{751}) mutated to alanine (4P-AS160), AS160 with arginine 973 mutated to lysine (RK-AS160), and AS160 with mutated Akt phosphorylation sites and R973K (4PRK-AS160) (4) were generously provided by Dr. G.E. Lienhard (Dartmouth Medical School, Hanover, NH). Hemagglutinin (HA)-tagged kinase-inactive Akt (AAA-Akt) with point mutations at Lys^{179}, Thr^{308}, and Ser^{473} (24) was a gift from Dr. J.R. Woodgett (Ontario Cancer Institute/Princess Margaret Hospital, Toronto, Ontario, Canada). HA-tagged α2-AMPK (α2-AMPK) was provided by Dr. L.A. Witters (Dartmouth Medical School). Chinese hamster ovary fibroblasts stably overexpressing the insulin receptor (CHO-IR) were from Dr. C. Yip (University of Toronto).

Cell culture and transfection. L6 myoblasts stably expressing GLUT4 with an exofacial *myc* epitope (L6 GLUT4*myc*) and CHO-IR cells were maintained in monolayer culture as previously described (24,25). Transfection of L6 GLUT4*myc* myoblasts grown on 25-mm glass coverslips and CHO-IR cells was performed using Lipofectamine 2000 (Invitrogen, Carlsbad, CA). All experiments were carried out at 18–24 h posttransfection. In CHO-IR and L6 cells, the transfection efficiency of the FLAG-AS160 constructs tested was ~80 and 40%, respectively. Expression levels in CHO-IR cells are shown in each figure. The expression of wild-type and mutant AS160 constructs in L6 cells was comparable, and surface GLUT4*myc* levels were quantified through single cell assays.

Immunoprecipitation and immunoblotting. CHO-IR cells expressing FLAG WT-AS160 were left unstimulated (basal) or stimulated with 100 nmol/l insulin, 50 ng/ml PDGF, 2 mmol/l AICAR, 0.5 mmol/l DNP, 0.45 mol/l sucrose, and 1 μmol/l 4-phorbol-12-myristate-13-acetate (PMA) in serum-free α-minimal essential media or incubated in HEPES-buffered saline in which 120 mmol/l K^+ gluconate isosmotically replaced NaCl at 37°C. Cells were lysed in buffer containing 30 mmol/l HEPES (pH 7.6), 150 mmol/l NaCl, 1% (vol/vol) Triton X-100, 1 mmol/l EDTA, 30 mmol/l $Na_4P_2O_7$, 25 mmol/l β-glycerophosphate, 10 mmol/l NaF, 1 mmol/l Na_3VO4, 100 nmol/l okadaic acid, and protease inhibitor cocktail (1 mmol/l benzamidine, 10 μmol/l E-64, 1 μmol/l leupeptin, and 0.2 mmol/l phenylmethylsulfonyl fluoride; Sigma-Aldrich, St. Louis, MO). AS160 was immunoprecipitated with a monoclonal anti-FLAG (1 μg antibody/mg protein; Sigma-Aldrich) rotating overnight at 4°C. A similar lysis and immunoprecipitation with anti-AS160 (Upstate Cell Signaling Solutions, Lake Placid, NY) was done with untransfected L6 cells. The immunocomplex and the supernatant were resuspended in Laemmli buffer containing β-mercaptoethanol and heated for 5 min at 95°C. Proteins were resolved on SDS-PAGE, transferred to PVDF membranes, and blocked with 5% milk. The immunocomplex was separated into two equal portions, each of which were immunoblotted with anti–phospho-Akt (pS/pT) substrate (Cell Signaling Technology, Beverly, MA) and anti-AS160 antibodies (a kind gift from Dr. G.E. Lienhard [2] or, in later experiments, from Upstate Cell Signaling Solutions). Membranes from the supernatants were incubated with anti-AS160, anti–phospho-Akt Ser^{473}, anti–phospho-Akt Thr^{308}, anti–phospho-AMPK Thr^{172} (Cell Signaling Technology), or anti-HA (BAbCO, Beverly, CA) antibodies. Membranes were washed in Tris-buffered saline with 0.02% Tween, incubated with horseradish peroxidase–conjugated secondary antibodies (Jackson Immunoresearch, West Grove, PA), visualized by enhanced chemiluminescence (Bio-Rad, Richmond, CA), and quantified using ImageJ software (National Institutes of Health, Bethesda, MD). Membranes were stripped by incubating in 62.5 mmol/l Tris-HCl, pH 6.7, 2% (wt/vol) SDS, and 100 mmol/l β-mercaptoethanol at 50°C, blocked in 5% milk, and reprobed with anti-AS160, anti-Akt1/2, or anti-AMPK antibodies.

Immunofluorescence confocal microscopy. Surface GLUT4*myc*, Akt phosphorylation, and actin remodeling were detected by indirect fluorescence microscopy as previously described (12) with slight modifications. Serum-starved L6 cells were unstimulated (basal) or stimulated with 100 nmol/l insulin, 50 ng/ml PDGF, 120 mmol/l K^+ gluconate, 1 μmol/l PMA, 2 mmol/l AICAR, 0.5 mmol/l DNP, or 0.45 mol/l sucrose at 37°C. Surface GLUT4*myc* was detected by incubating intact cells with anti-myc antibody (1:200) (Sigma-Aldrich) followed by Alexa 488–conjugated goat anti-rabbit IgG (1:750) (Molecular Probes, Eugene, OR) fixed with 4% paraformaldehyde and permeabilized with 0.1% (vol/vol) Triton X-100. Cells expressing epitope-tagged proteins were identified by immunostaining with the appropriate primary antibodies (monoclonal anti-FLAG antibody [1:5,000], polyclonal anti-FLAG antibody [1:750], or monoclonal anti-HA antibody [1:3,000]) followed by Cy3- or Cy5-conjugated anti-mouse or anti-rabbit IgG (1:750) (Jackson Immunoresearch). To assess actin remodeling or Akt phosphorylation, cells were unstimulated (basal) or stimulated with insulin or PDGF, fixed with 4% paraformaldehyde, permeabilized with 0.1% (vol/vol) Triton X-100, and incubated with rhodamine-conjugated phalloidin (Molecular Probes) or anti–phospho-Akt Ser^{473} immunohistochemistry-compatible antibody (Cell Signaling Technology) followed by Alexa 488–conjugated goat anti-rabbit IgG (1:750) as previously described (12). Fluorescent images were obtained with a Zeiss LSM 510 laser-scanning confocal microscope. Whole cells were scanned along the z-axis, and a single composite image (collapsed *xy* projection) of the optical cuts per cell was generated using LSM5 Image software. Surface GLUT4*myc* was quantified using ImageJ software (National Institutes of Health).

Statistical analyses. Statistical analyses were performed with one-way ANOVA (SigmaStat, Chicago, IL). Tukey post hoc comparisons were made when statistical significance ($P < 0.05$) was found between observations. Data are presented as means ± SE.

RESULTS

AS160 links insulin and PDGF to GLUT4*myc* translocation. While the increase in surface GLUT4 induced by PDGF occurs in parallel to Akt activation (12,13), it was not known if Akt activation is required for this outcome. Here, surface GLUT4*myc* was quantified in L6 myoblasts transfected with a kinase-inactive Akt mutant (AAA-Akt) (24). Surface GLUT4*myc* levels in unstimulated cells were unaffected by AAA-Akt, but PDGF-induced GLUT4*myc* exocytosis was reduced by 87 ± 2% (Fig. 1).

AS160 phosphorylation is typically detected from the reactivity of a 160-kDa band with the PAS antibody (3–6). Using this approach, we observed an insulin-dependent phosphorylation of a 160-kDa band in L6 cells (results not shown). To specifically define whether PDGF increases AS160 phosphorylation, we measured phosphorylation of transfected WT-AS160 in CHO-IR cells, which exhibit high transfection efficiency. PDGF and insulin treatments elevated AS160 phosphorylation by 3.2 ± 0.8- and 6.6 ± 0.9-fold, respectively (Fig. 2). These responses were prevented by preincubation with the PI3K inhibitor LY294002 (data not shown). We therefore explored whether AS160 is a component of the signaling cascade in PDGF-induced GLUT4 translocation. In control cells, insulin and PDGF raised surface GLUT4*myc* by 2.1 ± 0.1- and 2.4 ± 0.2-fold, respectively (Fig. 3*E*). In unstimulated cells, WT-AS160 reduced surface GLUT4*myc* (Fig. 3*A* and *E*); however, it did not affect the gain in surface GLUT4*myc* upon insulin or PDGF stimulation (Fig. 3*A* and *E*). In unstimulated cells expressing 4P-AS160, surface GLUT4*myc* was lower compared with control (Fig. 3*B* and *E*). However, 4P-AS160

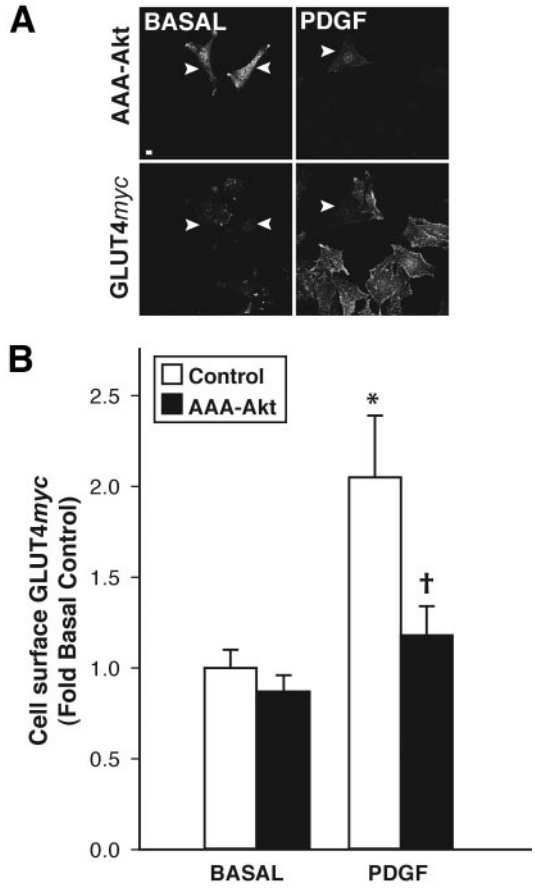

FIG. 1. Kinase-inactive Akt (AAA-Akt) abolishes PDGF-induced gain in cell-surface GLUT4*myc* in L6 myoblasts. L6 GLUT4*myc* myoblasts were transiently transfected with HA-AAA-Akt, then serum deprived and left unstimulated (BASAL) or stimulated with 50 ng/ml PDGF (7 min). Cell-surface GLUT4*myc* content was measured by detection of anti-*myc* antibody immunoreactivity in fixed nonpermeabilized cells using confocal fluorescence microscopy and quantified with ImageJ software, as described in RESEARCH DESIGN AND METHODS. Transfected cells were identified following permeabilization with 0.1% Triton-X100 and incubation with anti-HA antibody. *A*: Representative immunofluorescence images (collapsed *xy* projections) of five independent experiments (25–76 cells per condition) showing surface GLUT4*myc* content (*bottom panels*) in untransfected cells (control) versus cells transfected (indicated by arrowheads) with AAA-Akt (*top panels*). *B*: Quantification of cell-surface GLUT4*myc* content. Data are means ± SE and are expressed relative to the values in basal control cells. **P* < 0.05 vs. basal control; †*P* < 0.05 vs. control (within treatment). Scale bar, 10 μm.

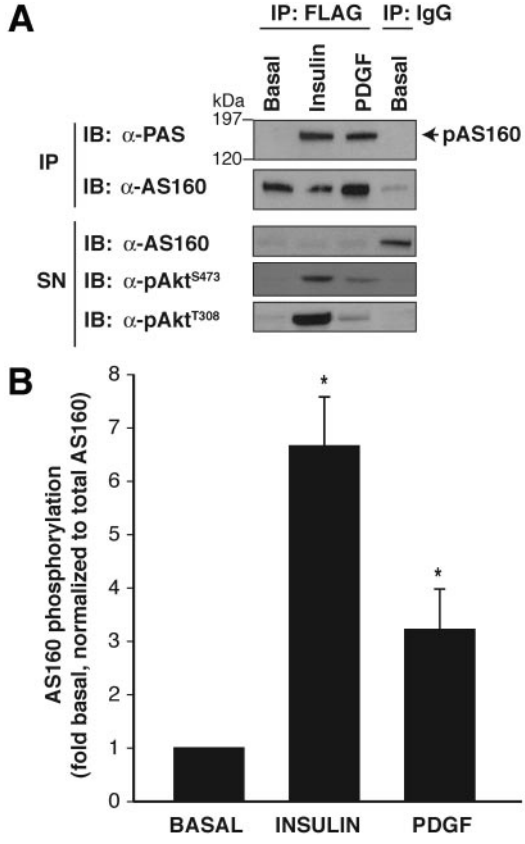

FIG. 2. AS160 phosphorylation is increased by insulin and PDGF stimulation in CHO-IR cells. FLAG-tagged WT-AS160 was transiently expressed in CHO-IR cells. AS160 was immunoprecipitated with anti-FLAG antibody from unstimulated (BASAL), insulin-treated (100 nmol/l, 10 min), or PDGF-treated (50 ng/ml, 7 min) CHO-IR cells. The immunocomplex (IP) and supernatant (SN) were separated by 7.5% or 10% SDS-PAGE. Membranes were blotted with anti–phospho-(Ser/Thr) Akt substrate (PAS), anti-AS160, or anti–phospho-Akt Ser^{473} or Thr^{308} antibodies. The same membranes were stripped and reprobed with anti-AS160 and anti-Akt antibodies (data not shown). Representative immunoblots (IB; *A*) and quantification of three to seven independent experiments (*B*) are shown. Data are means ± SE, expressed relative to basal, and are corrected by dividing the PAS densitometric signals by the respective densitometric signals of AS160. **P* < 0.05 vs. basal.

fully prevented GLUT4*myc* translocation triggered by insulin or PDGF (Fig. 3*B* and *E*). The observation that 4P-AS160 expression reduced surface GLUT4*myc* levels in nontreated cells complicates interpretation of the effects of 4P-AS160 on the multiple stimuli to increase surface GLUT4*myc*. In light of this, we calculated the net gains in surface GLUT4*myc* by subtracting the increase in response to each stimulus from the respective basal. These calculations reveal an action of the mutant on the actual responses and no longer include the residual effect of 4P-AS160 in the unstimulated state. In cells expressing 4P-AS160, the net gains in surface transporters in response to insulin or PDGF remained markedly lower compared with control (Fig. 3*E*, *inset*). In contrast, the insulin- or PDGF-stimulated gains in surface GLUT4*myc* were unaffected by RK-AS160 or 4PRK-AS160. Moreover, in the basal state, surface GLUT4*myc* levels were not diminished by RK-AS160 or 4PRK-AS160 and were similar to those observed in control cells (Fig. 3*C–E*). The observed reduction in surface GLUT4*myc* in unstimulated cells expressing WT-AS160 or 4P-AS160 is likely due to the augmented cellular Rab-GAP activity from the overexpressed protein. This interpretation is supported by the reciprocal observation that knockdown of endogenous AS160 in 3T3-L1 adipocytes by siRNA increases plasma membrane GLUT4 levels by enhancing the basal GLUT4 recycling rate (3,6).

Additional experiments demonstrated that insulin- or PDGF-induced Akt phosphorylation was unaffected by 4P-AS160 transfection (Fig. 4*A*). Similarly, 4P-AS160 did not influence insulin- or PDGF-regulated actin remodeling (Fig. 4*B*). Thus, the inhibitory effects of 4P-AS160 on insulin- or PDGF-stimulated GLUT4*myc* translocation did not result from 4P-AS160 sequestering Akt ot disrupting insulin-induced actin remodeling, a phenomenon that is Akt independent yet essential for insulin-dependent GLUT4 translocation (23,24).

AS160 is a component of c/n PKC signaling to GLUT4. Muscle contraction/exercise stimulates glucose uptake, an effect that may rely upon activation of AMPK, c/n PKC, and/or CaMK (20). Similarly, K^+ depolarization (14) and

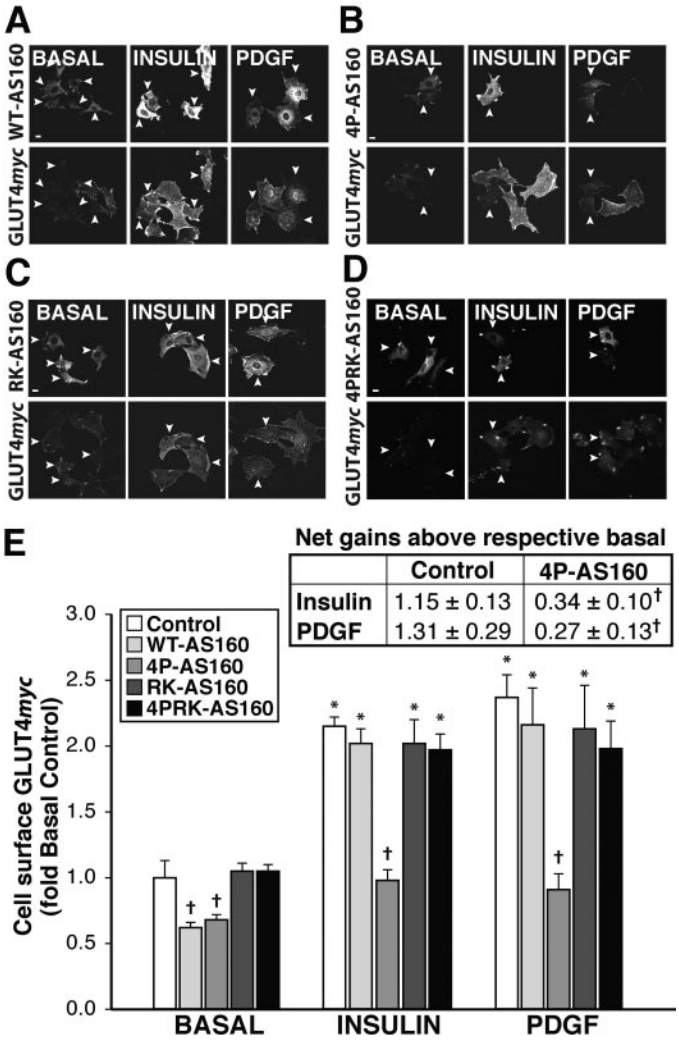

FIG. 3. Increased surface GLUT4*myc* elicited by insulin or PDGF in L6 myoblasts is reduced by 4P-AS160. Serum-deprived L6 GLUT4*myc* myoblasts transfected with the indicated constructs were left unstimulated (BASAL) or stimulated with either 100 nmol/l insulin (10 min) or 50 ng/ml PDGF (7 min). Cell-surface GLUT4*myc* content and transfected cells were detected as described in RESEARCH DESIGN AND METHODS *A–D*: Representative immunofluorescence images (collapsed *xy* projections) of surface GLUT4*myc* (*bottom panels*) in untransfected cells (control) versus cells transfected (indicated by arrowheads) with WT-AS160, 4P-AS160, RK-AS160, or 4PRK-AS160 (*top panels*). *E*: Quantification of cell-surface GLUT4*myc* content from 5 to 12 independent experiments (>100 cells per condition). Data are means ± SE and are expressed relative to the values in basal control cells. Table (*inset*) shows means ± SE of the net gain in surface GLUT4*myc* subtracted from the respective basal values. *$P < 0.05$ vs. basal control; †$P < 0.05$ vs. control (within treatment). Scale bar, 10 μm.

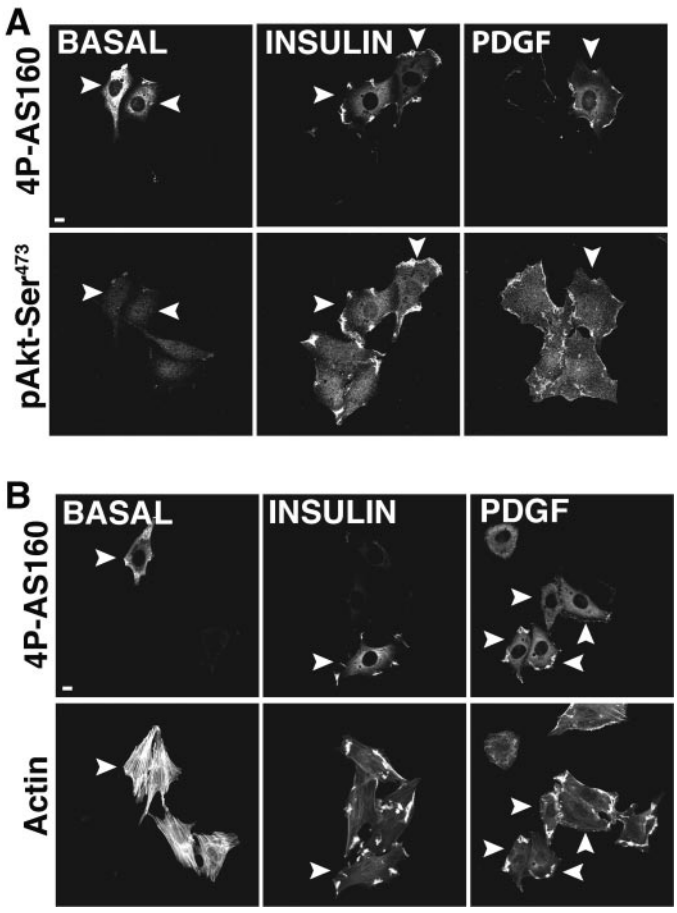

FIG. 4. 4P-AS160 does not affect insulin or PDGF-stimulated Akt Ser^{473} phosphorylation and actin remodeling in response to insulin or PDGF in L6 myoblasts. L6 GLUT4*myc* myoblasts were transfected with the indicated constructs, then serum deprived and left unstimulated (BASAL) or stimulated with either 100 nmol/l insulin (10 min) or 50 ng/ml PDGF (7 min). Akt Ser^{473} phosphorylation and filamentous actin were assessed by confocal fluorescence microscopy with an immunohistochemistry compatible anti–Akt Ser^{473} antibody and rhodamine-phallodin, respectively. Cells transfected (indicated by arrowheads) with 4P-AS160 (*top panels*) were identified as described in RESEARCH DESIGN AND METHODS. Shown are composite images of Akt Ser^{473} phosphorylation (*A*; collapsed *xy* projections, *bottom panels*) and actin remodeling (*B*; dorsal plane, *bottom panels*) of three independent experiments (30–60 cells per condition). Scale bar, 10 μm.

hyperosmolarity (16) also increase surface GLUT4*myc* in L6 cells. However, these effects of K^+ depolarization and hyperosmolarity occur independently of the PI3K and AMPK pathways (14,16,17) and may involve the participation of c/n PKC instead (14,21). Moreover, phorbol esters, which activate c/n PKC, promote GLUT4 exocytosis (26) and glucose uptake (27,28). Thus, we assessed if these activators of c/n PKC would increase AS160 phosphorylation and if AS160 is downstream of these signaling cascades that raise surface GLUT4*myc* content.

In CHO-IR cells, AS160 phosphorylation was elevated by K^+ depolarization (2.6 ± 0.4-fold), PMA (5.1 ± 0.6-fold), and hyperosmolar sucrose (6.7 ± 1.1-fold) (Fig. 5). Pretreatment of cells with bisindolylmaleimide (BIM), at concentrations (1 μmol/l) that only inhibit c/n PKC, reduced AS160 phosphorylation elicited by these stimuli (Fig. 5). Akt phosphorylation was unaffected by these stimuli (Fig. 5).

We next evaluated if the gain in surface GLUT4*myc* observed with these stimuli engages AS160 in L6 cells. Surface GLUT4*myc* levels were increased by K^+ depolarization (1.6 ± 0.1-fold), PMA (2.0 ± 0.2-fold), or hyperosmolar sucrose (2.3 ± 0.1-fold) (Fig. 6*A* and *E*). WT-AS160, RK-AS160, or 4PRK-AS160 did not alter the increased membrane GLUT4*myc* elicited by these stimuli (Fig. 6*A*, *D*, and *E*). In contrast, 4P-AS160 fully prevented the gain in surface GLUT4*myc* stimulated by K^+ depolarization and partly but significantly reduced the gains evoked by PMA and hyperosmolarity (Fig. 6*B* and *E*). The net gains in GLUT4*myc* in response to K^+ depolarization and PMA, but not to hyperosmolar sucrose, remained significantly lower in cells expressing 4P-AS160 (Fig. 6*E*, *inset*).

AS160 links the AMPK pathway to GLUT4*myc* translocation. In skeletal muscle or muscle cells, AMPK activation promotes GLUT4 exocytosis (17,29). AMPK exists

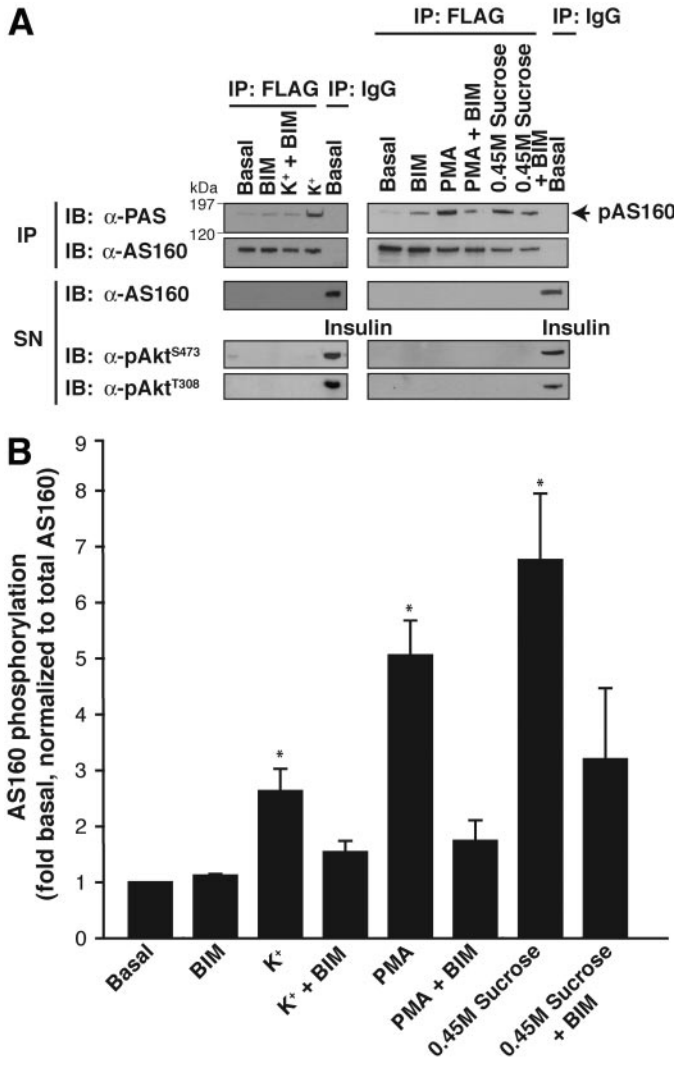

FIG. 5. AS160 phosphorylation is increased by stimuli that activate c/n PKC in CHO-IR cells. AS160 was immunoprecipitated with a monoclonal anti-FLAG antibody from CHO-IR cells transiently expressing FLAG WT-AS160 that were either not treated (Basal) or treated with 120 mmol/l K^+ gluconate (20 min), 1 μmol/l PMA (30 min), or 0.45 mol/l hyperosmolar sucrose (30 min), with or without a 30-min pretreatment with 1 μmol/l BIM (present continuously during the treatment periods). The immunocomplex (IP) and supernatant (SN) were separated by 7.5 or 10% SDS-PAGE. Membranes were blotted with anti-PAS, anti-AS160, or anti–phospho-Akt Ser^{473} or Thr^{308} antibodies. The same membranes were stripped and reprobed with anti-AS160 and anti-Akt antibodies (data not shown). Representative immunoblots (*A*) and quantification of three to nine independent experiments (*B*) are shown. Data are means ± SE, expressed relative to basal, and are normalized for AS160 expression by dividing the PAS densitometric signals by the respective densitometric signals of AS160. *$P < 0.05$ vs. basal.

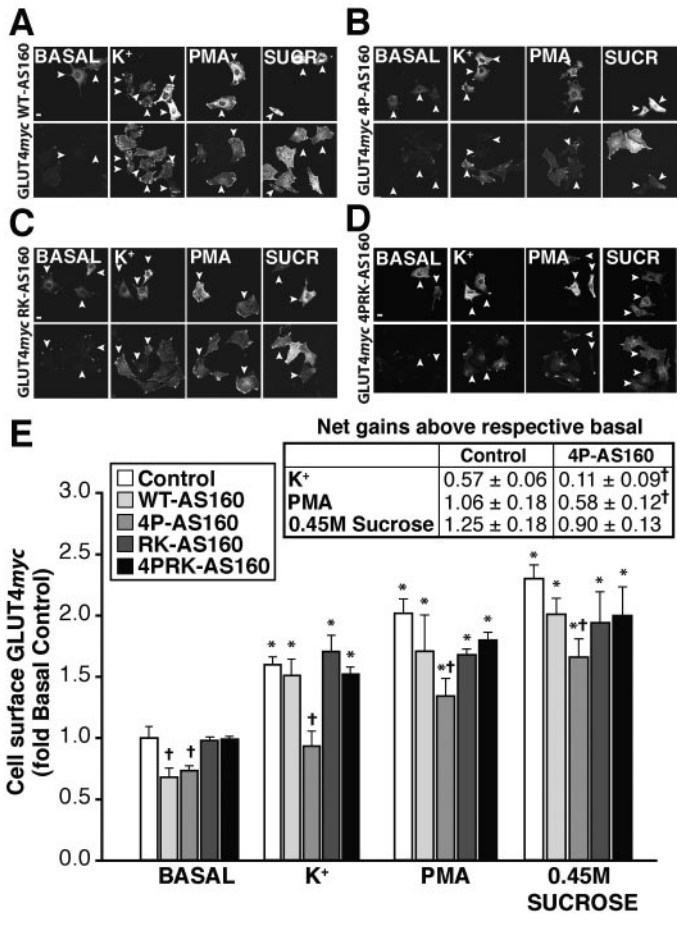

FIG. 6. Increased surface GLUT4*myc* elicited by stimuli acting via c/n PKC is reduced by 4P-AS160 in L6 myoblasts. L6 GLUT4*myc* myoblasts were transfected with the indicated constructs, then serum deprived and left unstimulated (BASAL) or stimulated with 120 mmol/l K^+ gluconate (20 min), 1 μmol/l PMA (30 min), or 0.45 mol/l hyperosmolar sucrose (30 min). Cell-surface GLUT4*myc* content and transfected cells were detected as described in RESEARCH DESIGN AND METHODS. *A–D*: Representative immunofluorescence images of surface GLUT4*myc* (*bottom panels*) in untransfected cells (control) versus cells transfected (indicated by arrowheads) with WT-AS160, 4P-AS160, RK-AS160, or 4PRK-AS160 (*top panels*). *E*: Quantification of cell-surface GLUT4*myc* of five to nine independent experiments (50–300 cells per condition). Data are means ± SE and are expressed relative to the values in basal control cells vicinal to transfected cells. Table (*inset*) shows means ± SE of the net gain in surface GLUT4*myc* subtracted from the respective basal values. *$P < 0.05$ vs. basal control; †$P < 0.05$ vs. control (within treatment). Scale bar, 10 μm.

as a heterotrimeric complex composed of α catalytic subunits with β and γ regulatory subunits (30). There are two isoforms of the catalytic subunit (α1 and -2); however, the stimulatory effects of AICAR (17,29) and hypoxia (19), but not hyperosmolarity (17), on glucose uptake requires α2-AMPK. Moreover, rodent skeletal muscle expresses more α2-AMPK, and a greater proportion of AMPK activity can be attributed to the α2-AMPK heterotrimeric complex (31).

We first assessed if α2-AMPK activation increases AS160 phosphorylation. In CHO-IR cells (which likely lack α2-AMPK), neither AICAR nor DNP caused WT-AS160 phosphorylation. However, upon transfection of α2-AMPK, WT-AS160 phosphorylation was increased by AICAR (2.7 ± 0.5-fold) or DNP (2.5 ± 0.3-fold) (Fig. 7). Conversely, hyperosmolar sucrose evoked WT-AS160 phosphorylation in CHO-IR cells, and this response was not further elevated by α2-AMPK transfection (Fig. 7). None of these stimuli affected Akt phosphorylation (Fig. 7).

We next explored if AS160 is a component of AMPK signaling leading to GLUT4 traffic. L6 cells express α2-AMPK, but total cellular AMPK activity is dominated by the α1-catalytic subunit (32). Since α2-AMPK mediates AICAR-stimulated glucose uptake in skeletal muscle (17,29) and α2-AMPK was required for AICAR- and DNP-stimulated AS160 phosphorylation in CHO-IR cells (Fig. 7), we cotransfected the α2-subunit with WT-AS160 or 4P-AS160 in L6 cells. In control cells, surface GLUT4*myc* density was raised by AICAR (2.0 ± 0.1-fold), DNP (1.6 ± 0.1-fold), and hyperosmolar sucrose (2.2 ± 0.1-fold) (Fig. 8*E*). The gains in surface transporters elicited by these

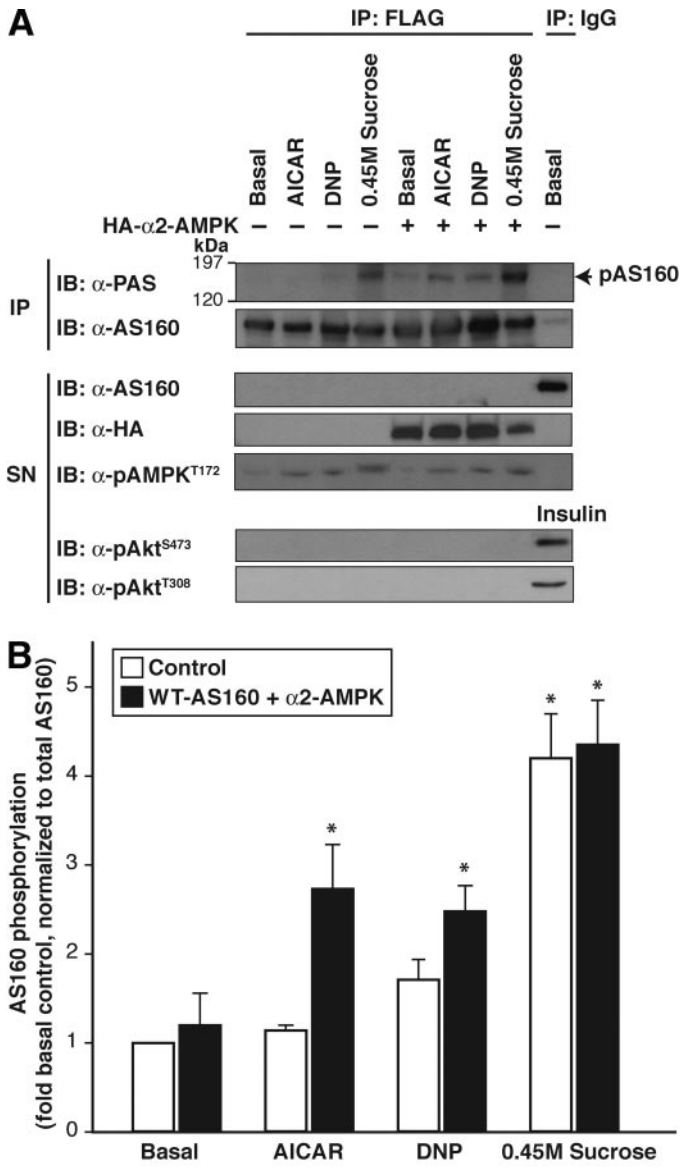

FIG. 7. AS160 phosphorylation is increased by activators of AMPK in CHO-IR cells only in the presence of the α2 catalytic subunit of AMPK. AS160 was immunoprecipitated with a monoclonal anti-FLAG antibody from CHO-IR cells transiently expressing FLAG WT-AS160 alone (control) or with cells expressing α2-AMPK that were unstimulated (Basal) or stimulated with AICAR (2 mmol/l, 40 min), DNP (0.5 mmol/l, 20 min), or hyperosmolar sucrose (0.45 mol/l, 30 min). The immunocomplex (IP) and supernatant (SN) were separated by 7.5 or 10% SDS-PAGE. Membranes were blotted with anti-PAS, anti-AS160, anti–phospho-Akt Ser^{473} or Thr^{308}, or anti–phospho-AMPK Thr^{172} antibodies. The same membranes were stripped and reprobed with anti-AS160, anti-Akt, or anti-AMPK antibodies (data not shown). Representative immunoblots (*A*) and quantification of three to nine independent experiments (*B*) are shown. Data are means ± SE, expressed relative to basal, and are normalized for AS160 expression by dividing the PAS densitometric signals by the respective AS160 densitometric signals. *$P < 0.05$ vs. basal.

stimuli were unaffected by WT-AS160, RK-AS160, or 4PRK-AS160 (Fig. 8*A* and *C–E*). In contrast, 4P-AS160 significantly reduced surface GLUT4*myc* in response to AICAR or DNP (Fig. 8*B* and *E*). In cells treated with hyperosmolar sucrose, 4P-AS160 modestly reduced surface GLUT4*myc* content (Fig. 8*B* and *E*) akin to that observed in the absence of α2-AMPK cotransfection (Fig. 6*B* and *E*). These data suggest that AS160 mediates GLUT4*myc* translocation in response to AICAR or DNP, especially in the context of higher α2-AMPK levels, but does not contribute to the rise in surface GLUT4 evoked by hyperosmolarity. The calculated net gains in GLUT4*myc* in response to AICAR, but not to either DNP or hyperosmolar sucrose, remained significantly lower in 4P-AS160–transfected cells (Fig. 8*E*, *inset*).

DISCUSSION

The identification of AS160 as an Akt substrate provides a link between insulin signaling and regulation of GLUT4 traffic. A current model proposes that the Rab-GAP activity of AS160 retains GLUT4 vesicles intracellularly in the basal state (3,6). This clamping action of AS160 on GLUT4 traffic is then relieved upon insulin stimulation through Akt phosphorylation, effectively uncoupling it from its regulation of a downstream Rab protein. The exact level or location at which insulin signaling pathways integrate with GLUT4 vesicle traffic is not clear, but recent studies suggest that in adipocytes, tethering and fusion of GLUT4 vesicles with the plasma membrane are a major regulated event (33,34) and that Akt activity is required for events beyond the arrival of vesicles near the membrane (34).

In addition to insulin, contraction increases the amount of GLUT4 at the plasma membrane (1,20). Intriguingly, these two stimuli require different early signal transduction pathways, since activation of class IA PI3K and Akt are not required for contraction-induced GLUT4 exocytosis or glucose uptake (20,35). Although contraction activates AMPK and activation of this enzyme by AICAR increases glucose uptake via GLUT4, there does not appear to be a causal role of AMPK in contraction-activated glucose uptake (17,19,20,29). Nonetheless, pathophysiological challenges such as hypoxia and DNP engage AMPK to stimulate glucose uptake (19). Moreover, AMPK has emerged as a viable pharmacological target in the treatment of type 2 diabetes (36,37), and chronic treatment of obese rodents with an AMPK activator improved glucose tolerance (38). The signals leading to the contraction-elicited GLUT4 exocytosis thus remain unknown, and there is circumstantial evidence suggesting that c/n PKC may participate in this response (28,39,40). Recently, we demonstrated that membrane depolarization, a prelude to muscle contraction, stimulates c/n PKC (21) and AMPK (14), but only the former mediates the depolarization stimulation of GLUT4 redistribution to the cell surface (14).

Given that such diverse stimuli increase surface GLUT4 levels in muscle cells, it was of interest to explore if the distinct signaling pathways engaged by the stimuli converge at a downstream step. Although AS160 was identified as an Akt substrate, examination of its linear sequence reveals putative phosphorylation sites by a variety of kinases, including AMPK and PKC. Hence, the purpose of this study was to examine if AS160 constitutes a convergence point in the increase in surface GLUT4 in muscle cells elicited by stimuli engaging three different signaling pathways (Akt, AMPK, and c/n PKC).

AS160 relays insulin and PDGF signaling to GLUT4. PDGF stands out due to its ability to activate Akt and GLUT4 translocation in cells that coexpress PDGF receptors and GLUT4 (12,13,41). Before the current research was undertaken, it was not known whether Akt is requisite to achieving GLUT4 externalization by PDGF. We show here that PDGF increased AS160 phosphorylation, and this effect was prevented by pretreatment with the PI3K inhib-

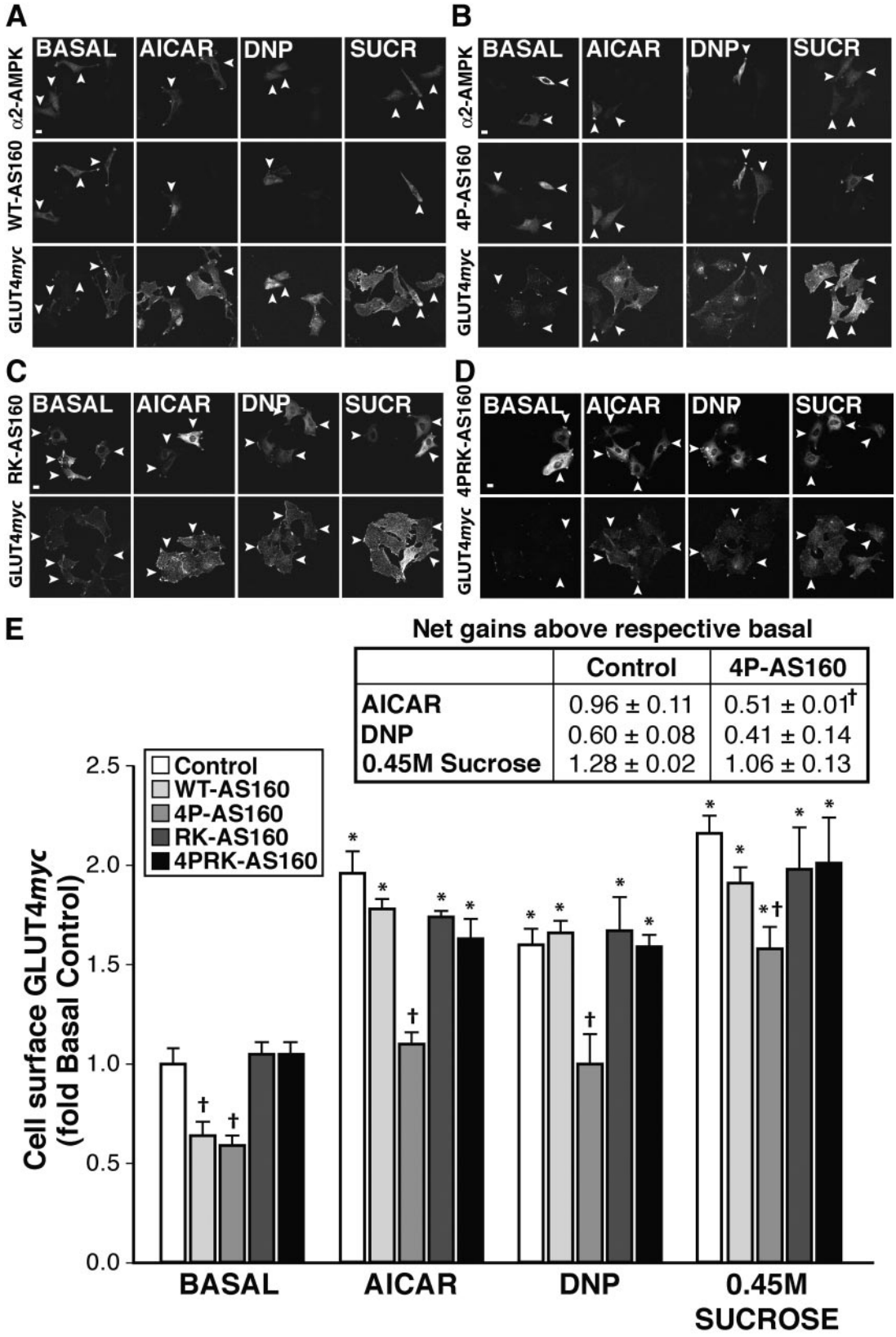

FIG. 8. Increased surface GLUT4*myc* elicited by stimuli that activate AMPK is reduced by 4P-AS160 in L6 myoblasts. L6 GLUT4*myc* myoblasts were transfected with the indicated constructs, then serum deprived and left unstimulated (BASAL) or stimulated with AICAR (2 mmol/l, 40 min), DNP (0.5 mmol/l, 20 min), or hyperosmolar sucrose (0.45 mol/l, 30 min). Cell-surface GLUT4*myc* and transfected cells were detected as described in Fig. 1. *A–D*: Representative immunofluorescence images of surface GLUT4*myc* (*bottom panels*) in cells expressing (indicated by arrowheads) α2-AMPK alone (control) or with WT-AS160, 4P-AS160, RK-AS160, or 4PRK-AS160 (*top panels*). *E*: Quantification of cell-surface GLUT4*myc* levels of five to eight independent experiments (53–94 cells per condition). Data are means ± SE and are expressed relative to the values in basal control cells. Table (*inset*) shows means ± SE of the net gain in surface GLUT4*myc* subtracted from the respective basal values. *$P < 0.05$ vs. basal control; †$P < 0.05$ vs. control (within treatment). Scale bar, 10 μm.

itor LY294002. Further, the gain in surface GLUT4 elicited by PDGF was abolished by a kinase-inactive Akt mutant. In addition, 4P-AS160 blocked the rise in surface GLUT4*myc* levels caused by PDGF, whereas RK-AS160 and 4PRK-AS160 (with inactive GAP activity) did not. Collectively, these results indicate that AS160 functionally participates not only in insulin- but also in PDGF-induced GLUT4 translocation in L6 cells downstream of PI3K.

AS160 phosphorylation was determined with the PAS antibody that recognizes the consensus Akt phosphorylation motif peptide sequence R*X*R*XX*(pS/pT). Intriguingly, this antibody also reacted with AS160 in cells treated with activators of α2-AMPK or c/n PKC, which do not stimulate Akt. Thus, AMPK and PKC can theoretically target the same AS160 sites phosphorylated by Akt and recognized by the PAS antibody. Indeed, of the six Akt phosphorylation sites, S318 (FRSRCSpSVTGV) and S588 (MRGRLGpSVDSF) have putative AMPK consensus phosphorylation motifs in the context φ *XX*R*XX*(pS/pT)*XXX*φ, where φ is a hydrophobic residue (42). In addition, S570 (KRSLTSpSLENI) has some features of an AMPK consensus phosphorylation motif, and five of the six Akt phosphorylation sites on AS160 fit the minimal PKC consensus phosphorylation motif, R*XX*pS (43). These observations prompted us to analyze the functional role of AS160 upon activation of AMPK and c/n PKC.

PKC activation leads to AS160 phosphorylation regulating GLUT4 traffic. Muscle contraction triggers PKC translocation to the plasma membrane (44), and this has been argued to be causally related to the observed increase in glucose uptake (40). Here we found that K^+ depolarization, PMA, and hyperosmolar sucrose all increased WT-AS160 phosphorylation. The c/n PKC inhibitor BIM prevented WT-AS160 phosphorylation evoked by K^+ depolarization and PMA and reduced that elicited by hyperosmolar sucrose, suggesting that these stimuli lead to AS160 phosphorylation at least in part through c/n PKC. 4P-AS160 expression abolished the rise in surface GLUT4*myc* triggered by K^+ depolarization. Intriguingly, however, 4P-AS160 only partially reduced the gain in surface GLUT4*myc* caused by PMA and minimally by hyperosmolar sucrose (Fig. 6*E*). Further studies will be required to identify the precise kinases and signals involved in PMA-induced GLUT4 translocation. However, our previous study (14) rules out AMPK and CaMKII as possible mediators of the K^+ depolarization response.

We previously demonstrated that K^+ depolarization largely increases surface GLUT4*myc* in L6 cells by inhibiting its endocytosis, possibly via activation of c/n PKC (14,21). Although AS160 is not required for insulin regulation of GLUT4 endocytosis in 3T3-L1 adipocytes (5), it is possible that AS160 might participate in regulating GLUT4 endocytosis in response to K^+ depolarization. In L6 cells, hyperosmolar sucrose also inhibits GLUT4 endocytosis (12). However, 4P-AS160 did not significantly affect the net gains in surface GLUT4*myc* induced by hyperosmolar sucrose. These data imply that inhibition of GLUT4 endocytosis by hyperosmolar sucrose is not mediated by AS160. Instead it is likely caused by hyperosmolar sucrose preventing clathrin-coated pit formation (45).

AS160 mediates signaling from AMPK to GLUT4. AS160 phosphorylation is increased by AICAR or muscle contraction in rodent muscle (8), and when this article was being prepared for publication, two studies (46,47) showed that α2-AMPK is responsible for the AICAR and possibly the contraction effects. DNP elevates surface GLUT4 and glucose uptake (14,16), and in L6 cells, this process is dependent on AMPK activity (14). Here we show that AICAR and DNP increase AS160 phosphorylation in CHO-IR cells, but only when the cells expressed α2-AMPK. Moreover, in L6 cells expressing α2-AMPK, 4P-AS160 largely prevented the AICAR- and DNP-induced increase in surface GLUT4*myc*.

However, when net gains in surface GLUT4*myc* were calculated, the AICAR response remained significant, whereas the DNP response was not significantly altered by 4P-AS160 (Fig. 8*E*). One interpretation is that AS160 is not a component mediating the stimulatory actions of DNP via AMPK or other signaling proteins on GLUT4 exocytosis. Alternatively, in addition to activating AMPK, DNP also raises intracellular Ca^{2+} (48), and in L6 cells, chelating intracellular Ca^{2+} reduced DNP-stimulated glucose uptake (16). AS160 has a Ca^{2+}/calmodulin binding domain, and its binding to AS160 has been proposed to disable its GAP activity (49). Thus, the inhibitory effect of 4P-AS160 on net gain in surface GLUT4*myc* in DNP-treated cells may have been opposed by Ca^{2+}/calmodulin binding to AS160, resulting in partial deactivation of its GAP activity.

AS160 as a signaling integrator and implications for diabetes. The results presented indicate that AS160 can be phosphorylated in response to agents activating Akt, c/n PKC, and AMPK. The specific sites phosphorylated in response to each stimulus must now be identified. The outcome of each of these phosphorylation events may depend on the site modified, as well as on the duration of the signal and localization of AS160. In this way, AS160 may integrate distinct signals that could conceivably control its GAP activity toward individual Rab proteins that may be associated with GLUT4 vesicle movement, tethering, or fusion with the plasma membrane (6,7).

While our results indicate that both insulin-dependent and -independent signaling cascades that mutually increase plasma membrane GLUT4 levels intersect at AS160, they do not suggest that AS160 is the end point in regulating GLUT4 traffic. Hence, the possibility exists that these signaling cascades may diverge from AS160 and subsequently target distinct downstream effectors to regulate GLUT4 traffic. It should also be considered that PKC and AMPK may phosphorylate AS160 on sites not recognized by the PAS antibody, and such phosphorylations may have additional functional effects on AS160 and GLUT4 traffic. Moreover, the fact that neither AS160 mutant with disabled GAP activity (RK or 4PRK) elevated surface GLUT4*myc* above levels observed in control cells suggests that AS160 is necessary but insufficient for GLUT4 traffic. It is also possible that these stimuli, like insulin (3,6), utilize both AS160-dependent and -independent mechanisms to promote a gain in surface transporters.

Exercise represents a viable mechanism to bypass insulin resistance of glucose uptake in obese and diabetic patients. Therefore, unraveling the signals elicited by exercise will be paramount in our ability to relieve insulin resistance. AMPK and c/n PKC have been implicated as partial contributors to exercise-stimulated glucose uptake. The present discovery (i.e., AS160 is downstream of c/n PKC and AMPK, leading to increases in surface GLUT4) makes AS160 a key target for modulation and improvement of insulin sensitivity. Future studies should consider strategies to deactivate AS160 for therapeutic purposes, specifically in the sites modified by Akt, c/n PKC, or AMPK.

ACKNOWLEDGMENTS

This work was supported by grant MT12601 from the Canadian Institutes of Health Research (CIHR) to A.K. F.S.L.T. was supported by postdoctoral research fellowships from Natural Sciences and Engineering Research Council of Canada and CIHR.

We are grateful to Dr. G.E. Lienhard for the AS160 cDNAs and anti-AS160 antibody, Dr. J.R. Woodgett for the AAA-Akt cDNA, Dr. L.A. Witters for the α2-AMPK cDNA, and Dr. C.C. Yip for the CHO-IR cells used in this study.

REFERENCES

1. Thong FSL, Dugani CB, Klip A: Turning signals on and off: GLUT4 traffic in the insulin-signaling highway. *Physiology* 20:271–284, 2005
2. Kane S, Sano H, Liu SCH, Asara JM, Lane WS, Garner CC, Lienhard GE: A method to identify serine kinase substrates: Akt phosphorylates a novel adipocyte protein with a rab GTPase-activating protein (GAP) domain. *J Biol Chem* 277:22115–22118, 2002
3. Eguez L, Lee A, Chavez JA, Miinea CP, Kane S, Lienhard GE, McGraw TE: Full intracellular retention of GLUT4 requires AS160 Rab GTPase activating protein. *Cell Metab* 2:263–272, 2005
4. Sano H, Kane S, Sano E, Miinea CP, Asara JM, Lane WS, Garner CW, Lienhard GE: Insulin-stimulated phosphorylation of a Rab GTPase-activating protein regulates GLUT4 translocation. *J Biol Chem* 278:14599–14602, 2003
5. Zeigerer A, McBrayer MK, McGraw TE: Insulin stimulation of GLUT4 exocytosis, but not its inhibition of endocytosis, is dependent on RabGAP AS160. *Mol Biol Cell* 15:4406–4415, 2004
6. Larance M, Ramm G, Stockli J, van Dam EM, Winata S, Wasinger V, Simpson F, Graham M, Junutula JR, Guilhaus M, James DE: Characterization of the role of the Rab GTPase-activating protein AS160 in insulin-regulated GLUT4 trafficking. *J Biol Chem* 280:37803–37813, 2005
7. Miinea CP, Sano H, Kane S, Sano E, Fukuda M, Peranen J, Lane WS, Lienhard GE: AS160, the Akt substrate regulating GLUT4 translocation, has a functional Rab GTPase-activating protein domain. *Biochem J* 391: 87–93, 2005
8. Bruss MD, Arias EB, Lienhard GE, Cartee GD: Increased phosphorylation of Akt substrate of 160 kDa (AS160) in rat skeletal muscle in response to insulin or contractile activity. *Diabetes* 54:41–50, 2005
9. Karlsson HKR, Zierath JR, Kane S, Krook A, Lienhard GE, Wallberg-Henriksson H: Insulin-stimulated phosphorylation of the Akt substrate AS160 is impaired in skeletal muscle of type 2 diabetic subjects. *Diabetes* 54:1692–1697, 2005
10. Plomgaard P, Bouzakri K, Krogh-Madsen R, Mittendorfer B, Zierath JR, Pedersen BK: Tumor necrosis factor-α induces skeletal muscle insulin resistance in healthy human subjects via inhibition of Akt substrate 160 phosphorylation. *Diabetes* 54:2939–2945, 2005
11. Ramm G, Larance M, Guilhaus M, James DE: A role for 14-3-3 in insulin-stimulated GLUT4 translocation through its interaction with the RabGAP AS160. *J Biol Chem* 281:29174–29180, 2006
12. Torok D, Patel N, JeBailey L, Thong FSL, Randhawa VK, Klip A, Rudich A: Insulin but not PDGF relies on actin remodeling and on VAMP2 for GLUT4 translocation in myoblasts. *J Cell Sci* 117:5447–5455, 2004
13. Yuasa T, Kakuhata R, Kishi K, Obata T, Shinohara Y, Bando Y, Izumi K, Kajiura F, Matsumoto M, Ebina Y: Platelet-derived growth factor stimulates glucose transport in skeletal muscles of transgenic mice specifically expressing platelet-derived growth factor receptor in the muscle, but it does not affect blood glucose levels. *Diabetes* 53:2776–2786, 2004
14. Wijesekara N, Tung A, Thong F, Klip A: Muscle cell depolarization induces a gain in surface GLUT4 via reduced endocytosis, independently of AMPK. *Am J Physiol Endocrinol Metab* 290:1276–1286, 2006
15. Wright DC, Hucker KA, Holloszy JO, Han DH: Ca^{2+} and AMPK both mediate stimulation of glucose transport by muscle contractions. *Diabetes* 53:330–335, 2004
16. Patel N, Khayat ZA, Ruderman NB, Klip A: Dissociation of 5′ AMP-activated protein kinase activation and glucose uptake stimulation by mitochondrial uncoupling and hyperosmolar stress: differential sensitivities to intracellular Ca^{2+} and protein kinase C inhibition. *Biochem Biophys Res Comm* 285:1066–1070, 2001
17. Fujii N, Hirshman MF, Kane EM, Ho RC, Peter LE, Seifert MM, Goodyear LJ: AMP-activated protein kinase α2 activity is not essential for contraction- and hyperosmolarity-induced glucose transport in skeletal muscle. *J Biol Chem* 280:39033–39041, 2005
18. Ryder JW, Yang J, Galuska D, Rincón J, Björnholm M, Krook A, Lund S, Pedersen O, Wallberg-Henriksson H, Zierath JR, Holman GD: Use of a novel impermeable biotinylated photolabeling reagent to assess insulin- and hypoxia-stimulated cell surface GLUT4 content in skeletal muscle from type 2 diabetic patients. *Diabetes* 49:647–654, 2000
19. Mu J, Brozinick JT Jr, Valladares O, Bucan M, Birnbaum MJ: A role for AMP-activated protein kinase in contraction- and hypoxia-regulated glucose transport in skeletal muscle. *Mol Cell* 7:1085–1094, 2001
20. Rose AJ, Richter EA: Skeletal muscle glucose uptake during exercise: how is it regulated? *Physiology* 20:260–270, 2005
21. Tung A, Wijesekara N, Klip A: A cellular model of depolarization-regulated GLUT4 exocytosis and endocytosis in muscle cells (Abstract). *FASEB J* 20:A1280, 2006
22. Deshmukh A, Coffey VG, Zhong Z, Chibalin AV, Hawley JA, Zierath JR: Exercise-induced phosphorylation of the novel Akt substrate AS160 and filamin in human skeletal muscle. *Diabetes* 55:1776–1782, 2006
23. Rudich A, Klip A: Push/pull mechanisms of GLUT4 traffic in muscle cells. *Acta Physiol Scand* 178:297–308, 2003
24. Wang Q, Somwar R, Bilan PJ, Liu Z, Jin J, Woodgett JR, Klip A: Protein kinase B/Akt participates in GLUT4 translocation by insulin in L6 myotubes. *Mol Cell Biol* 19:4008–4018, 1999
25. Wang Q, Bilan PJ, Klip A: Opposite effects of insulin on focal adhesion proteins in 3T3–L1 adipocytes and in cells overexpressing the insulin receptor. *Mol Biol Cell* 9:3057–3069, 1998
26. Holman GD, Kozka IJ, Clark AE, Flower CJ, Saltis J, Habberfield AD, Simpson IA, Cushman SW: Cell surface labeling of glucose transporter isoform GLUT4 by bis- mannose photolabel: correlation with stimulation of glucose transport in rat adipose cells by insulin and phorbol ester. *J Biol Chem* 265:18172–18179, 1990
27. Hansen PA, Corbett JA, Holloszy JO: Phorbol esters stimulate muscle glucose transport by a mechanism distinct from the insulin and hypoxia pathways. *Am J Physiol Endocrinol Metab* 273:E28–E36, 1997
28. Henriksen EJ, Rodnick KJ, Holloszy JO: Activation of glucose transport in skeletal muscle by phospholipase C and phorbol ester: evaluation of the regulatory roles of protein kinase C and calcium. *J Biol Chem* 264:21536–21543, 1989
29. Jorgensen SB, Viollet B, Andreelli F, Frosig C, Birk JB, Schjerling P, Vaulont S, Richter EA, Wojtaszewski JFP: Knockout of the α2 but not α1 5′-AMP-activated protein kinase isoform abolishes 5-aminoimidazole-4-carboxamide-1-β-4-ribofuranoside but not contraction-induced glucose uptake in skeletal muscle. *J Biol Chem* 279:1070–1079, 2004
30. Woods A, Cheung PCF, Smith FC, Davison MD, Scott J, Beri RK, Carling D: Characterization of AMP-activated protein kinase beta and gamma subunits: assembly of the heterotrimeric complex in vitro. *J Biol Chem* 271:10282–10290, 1996
31. Cheung PC, Salt IP, Davies SP, Hardie DG, Carling D: Characterization of AMP-activated protein kinase gamma-subunit isoforms and their role in AMP binding. *Biochem J* 346:659–669, 2000
32. Konrad D, Rudich A, Bilan PJ, Patel N, Richardson C, Witters LA, Klip A: Troglitazone causes acute mitochondrial membrane depolarisation and an AMPK-mediated increase in glucose phosphorylation in muscle cells. *Diabetologia* 48:954–966, 2005
33. van Dam EM, Govers R, James DE: Akt activation is required at a late stage of insulin-induced GLUT4 translocation to the plasma membrane. *Mol Endocrinol* 19:1067–1077, 2005
34. Lizunov VA, Matsumoto H, Zimmerberg J, Cushman SW, Frolov VA: Insulin stimulates the halting, tethering, and fusion of mobile GLUT4 vesicles in rat adipose cells. *J Cell Biol* 169:481–489, 2005
35. Sakamoto K, Arnolds DE, Fujii N, Kramer HF, Hirshman MF, Goodyear LJ: Role of Akt2 in contraction-stimulated cell signaling and glucose uptake in skeletal muscle. *Am J Physiol Endocrinol Metab* 291:E1031–E1037, 2006
36. Musi N, Goodyear LJ: Insulin resistance and improvements in signal transduction. *Endocrine* 29:73–80, 2006
37. Barnes BR, Zierath JR: Role of AMP-activated protein kinase in the control of glucose homeostasis. *Curr Mol Med* 5:341–348, 2005
38. Cool B, Zinker B, Chiou W, Kifle L, Cao N, Perham M, Dickinson R, Adler A, Gagne G, Iyengar R, Zhao G, Marsh K, Kym P, Jung P, Camp HS, Frevert E: Identification and characterization of a small molecule AMPK activator that treats key components of type 2 diabetes and the metabolic syndrome. *Cell Metab* 3:403–416, 2006
39. Ihlemann J, Galbo H, Ploug T: Calphostin C is an inhibitor of contraction, but not insulin-stimulated glucose transport, in skeletal muscle. *Acta Physiol Scand* 167:69–75, 1999
40. Cleland PJ, Appleby GJ, Rattigan S, Clark MG: Exercise-induced translocation of protein kinase C and production of diacylglycerol and phosphatidic acid in rat skeletal muscle in vivo: relationship to changes in glucose transport. *J Biol Chem* 264:17704–17711, 1989
41. Whiteman EL, Chen JJ, Birnbaum MJ: Platelet-derived growth factor

(PDGF) stimulates glucose transport in 3T3–L1 adipocytes overexpressing PDGF receptor by a pathway independent of insulin receptor substrates. *Endocrinology* 144:3811–3820, 2003
42. Weekes J, Ball KL, Caudwell FB, Hardie DG: Specificity determinants for the AMP-activated protein kinase and its plant homologue analysed using synthetic peptides. *FEBS Lett* 334:335–339, 1993
43. Pearson RB, Kemp BE: Protein kinase phosphorylation site sequences and consensus specificity motifs: tabulations. *Methods Enzymol* 200:62–81, 1991
44. Richter EA, Cleland PJ, Rattigan S, Clark MG: Contraction-associated translocation of protein kinase C in rat skeletal muscle. *FEBS Lett* 217:232–236, 1987
45. Heuser JE, Anderson RG: Hypertonic media inhibit receptor-mediated endocytosis by blocking clathrin-coated pit formation. *J Cell Biol* 208:389–400, 1989
46. Treebak JT, Glund S, Deshmukh A, Klein DK, Long YC, Jensen TE, Jorgensen SB, Viollet B, Andersson L, Neumann D, Wallimann T, Richter EA, Chibalin AV, Zierath JR, Wojtaszewski JFP: AMPK-mediated AS160 phosphorylation in skeletal muscle is dependent on AMPK catalytic and regulatory subunits. *Diabetes* 55:2051–2058, 2006
47. Kramer HF, Witczak CA, Fujii N, Jessen N, Taylor EB, Arnolds DE, Sakamoto K, Hirshman MF, Goodyear LJ: Distinct signals regulate AS160 phosphorylation in rfesponse to insulin, AICAR, and contraction in mouse skeletal muscle. *Diabetes* 55:2067–2076, 2006
48. Hudman D, Rainbow RD, Lawrence CL, Standen NB: The origin of calcium overload in rat cardiac myocytes following metabolic inhibition with 2,4-dinitrophenol. *J Mol Cell Cardiol* 34:859–871, 2002
49. Kane S, Lienhard GE: Calmodulin binds to the Rab GTPase activating protein required for insulin-stimulated GLUT4 translocation. *Biochem Biophys Res Commun* 335:175–180, 2005